

A00-36686

AIAA 00-3486 Experimental Investigation of a 2-D MHD Slipstream Accelerator and Generator

E.D. Meloney, M.A.S. Minucci, L.N. Myrabo, H.T. Nagamatsu, and R.M. Bracken Department of Mechanical Engineering, Aeronautical Engineering, and Mechanics Rensselaer Polytechnic Institute Troy, NY

36th Joint Propulsion Conference and Exhibit 16–19 July 2000 Huntsville, Alabama

EXPERIMENTAL INVESTIGATION OF A 2-D MHD SLIPSTREAM ACCELERATOR AND GENERATOR

E.D. Meloney*, M.A.S. Minucci[†], L.N. Myrabo[‡], H.T. Nagamatsu[§], and R.M. Bracken[¶]
Department of Mechanical Engineering, Aeronautical Engineering, and Mechanics
Rensselaer Polytechnic Institute
Trov. New York 12180

ABSTRACT

An experimental study of the magnetohydrodynamic (MHD) effects of partially dissociated and ionized flow over an 80-degree included angle wedge with a 0.3 Tesla permanent magnet is presently being undertaken in the Rensselaer Polytechnic Institute 24-inch Hypersonic Shock Tunnel. The selected flow freestream conditions are approximately Mach 7.6, 4100 K (7380 R) stagnation temperature, and 780 psia stagnation pressure. In the initial part of the study, the power generation characteristics of the flow were investigated to determine the conductivity of the flow through the MHD channel. The generator results have been The next phase of study involves the establishment of an electric discharge between the electrodes of the same model to accelerate the plasma. Initial calculations have revealed that at least 30 kW of energy must be added to the flow to see a 1 psia increase in impact pressure behind the MHD With initial planning completed, the instrumentation and equipment is being built and acquired for this second stage of research.

INTRODUCTION

In the 1960's the interaction of high velocity plasma with a magnetic field was actively investigated by a number of researchers, including

Graduate Student, AIAA Student Member

Rosa, ¹ 1962, Nagamatsu & Sheer, ² 1961, Nagamatsu ³ et al., 1962, Way ⁴ et al, 1961, and Steg & Sutton, ⁵ 1960. This interest in magneto-hydrodynamic (MHD) phenomena arose from applications in thermonuclear reactions, astrophysics, electric power generation, space propulsion, and the magneto-aerodynamic control of ICBM nose cones (Ericson ⁶ et al, 1962) and the Apollo re-entry capsule. Until recently, numerous analytical but only limited experimental papers were published on hypersonic MHD phenomena.

Presently, interest in MHD for aerospace applications has been renewed by the need to drastically decrease the cost of launching payloads to space (Covault, 1999, Gurijanov et al, 1996). Myrabo et al. (1995) have proposed that laser or microwave beams could power a MHD slipstream accelerator to propel vehicles, called Lightcraft, to an orbital Mach number of 25 and potentially reduce launch costs by a factor of 100 to 1000, as compared to today's chemical rocket launchers.

The interest in developing a hypersonic MHD airbreathing propulsion system motivated the present investigation. Two different geometries for hypersonic MHD and slipstream accelerators have recently been investigated in the Rensselaer Polytechnic Institute 24-inch Hypersonic Shock Tunnel. The first model, which is axisymmetric and fitted with 24 peripheral open-top MHD channels and two pulsed Bitter-type electromagnetic coils was successfully tested at Mach 7.8 (Kerl^{10, 11} et al, 1999). The test program was designed to first demonstrate MHD power extraction from the hypersonic inlet flow, then MHD acceleration of the inlet flow. The Shock Tunnel generated the 4100 K (7380 R) and 780 psia reservoir of air necessary for adequate electrical conductivity behind the conical shock wave. The first tests indicated that the hypersonic airflow past the channels was indeed decelerated because of the interaction of the high speed, high temperature airflow in the channels and the perpendicular pulsed magnetic field. Laser-based

[†] Invited Visiting Research Scientist, Brazilian Air Force Major, AIAA Senior Member

^{*} Associate Professor of Engineering Physics, AIAA Senior Member

[§] Active Professor Emeritus of Aeronautical Engineering, AIAA

[¶] Graduate Student, AIAA Student Member

Copyright © 2000 by E.D. Meloney and L. N. Myrabo. Published by the American Institute of Aeronautics and Astronautics, Inc., with permission.

schlieren and luminosity photographs confirmed this flow deceleration due to energy extraction in the MHD channels. The extracted voltage was also recorded as a function of the external electrical load. Unfortunately, due to model complexity and the lack of a suitable electrode power supply, acceleration of the conducting airflow past the MHD channels could not be attempted. To overcome this problem, therefore, a second slipstream accelerator model with 2-D geometry, a single open-top MHD channel, and permanent Nd-Fe-B magnets is presently being investigated in the RPI facility (Fig. 8). The 2-D MHD accelerator model testing preparations are the subject of the present paper.

RPI 61-CM HYPERSONIC SHOCK TUNNEL

The 2-D MHD Slipstream Accelerator model tests are being conducted in the Rensselaer Polytechnic Institute 61-cm Hypersonic Shock Tunnel. Fig. 1 is a photograph of the Hypersonic Shock Tunnel. A detailed description of the tunnel facility can be found elsewhere (Minucci, 12 1991, Minucci, 13 et al., 1994).

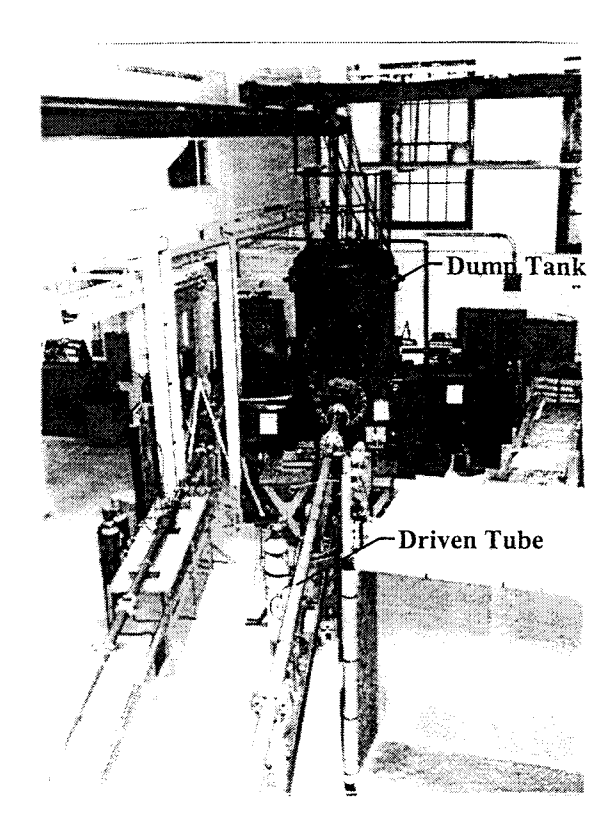


Fig. 1 Rensselaer Polytechnic 61-cm Hypersonic Shock Tunnel

For the present investigation, the tunnel was operated in the equilibrium interface mode near

ambient temperature (Minucci¹³ et al., 1994), using argon as the gaseous piston (Nascimento^{14, 15} et al., 1997,1998), helium as the driver gas, and air as the test gas. In this mode of operation, the RPI facility can generate high enthalpy reservoir conditions—4100 K temperature and 780 psia pressure—upstream of the nozzle entrance for approximately 2 ms. By selecting the appropriate throat diameter, a free stream Mach 7.6 airflow is produced in the test section. The combination of high enthalpy reservoir conditions and free stream Mach number, in turn, assure the minimum necessary electrical conductivity of air flowing behind the attached shock wave that stands around the model during the 2 ms of useful test time.

The Maxwell capacitor bank in Fig. 2 was donated by the U.S. Army to the RPI Hypersonic Laboratory and provided the high current, high voltage pulse that drove the two Bitter-type coils inside the axisymmetric MHD slipstream accelerator model¹⁰. The authors' original intentions were to use this same capacitor bank as the high-voltage power supply needed to drive the flow-accelerating current between the wedge accelerator model electrodes.

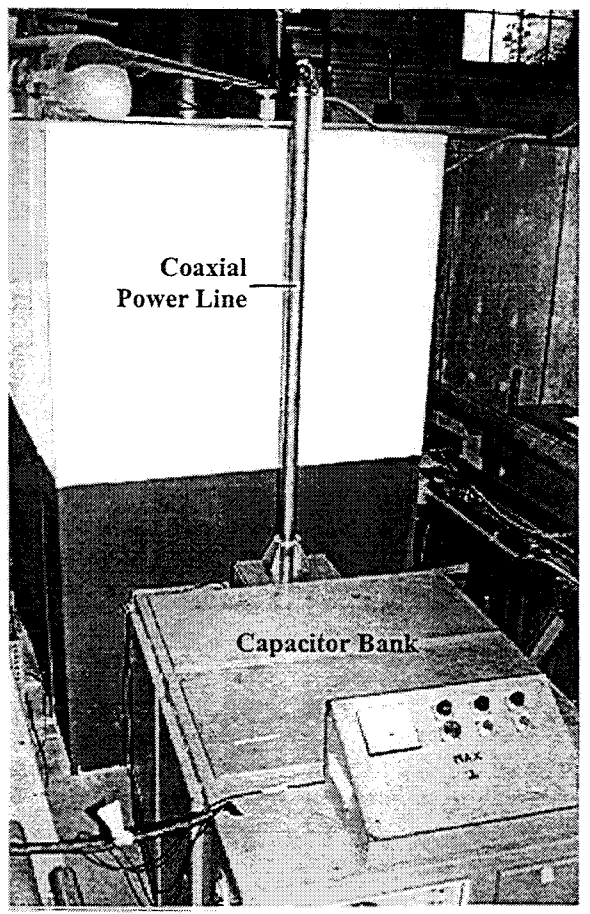


Fig. 2 Maxwell Capacitor Bank and Coaxial Power Line

Tektronix VXI and Test Lab data acquisition systems record pressure data from PCB piezoelectric transducers, shock tunnel heat transfer gauge signals, and the electric current and voltage readings from the electrode power supply discharge. A computer code written for LabVIEWTM software serves as the interface between researchers and the acquired data and acquisition equipment. Fig. 3 is a schematic drawing of the end of the Hypersonic Shock Tunnel driven section indicating the apparatus described.

A Beckman & Whitley Inc. model 350 framing drum camera, on loan from the NASA Marshall Space Flight Center, has been modified to also serve as a high-speed open-shutter drum camera. A recently acquired Oxford Lasers 'n-Shot Controller' is used to accurately time the pulses from the laser, which allows the camera to be properly used in an open-shutter mode. This new piece of equipment also adds a great deal of flexibility to the timing and triggering setup of the shock tunnel. In this mode, the camera can be operated in conjunction with the timed pulses of the copper vapor laser to

provide a series of 35mm schlieren photographs during the test time. By scanning and assembling the photos, schlieren movies can then be produced which greatly enhance the value of the visual data. In addition, simple digital enhancements can be made to help further clarify the shock waves.

EXPERIMENTAL APPARATUS

The electrode power supply is connected to the shock tunnel test section via a copper coaxial power line (Fig. 2). An in-house designed and built ceramic feed-through plate enables the power line to pass, isolated, through the test section steel wall before connecting to the model (Fig. 4). During the axisymmetric MHD model tests, the coaxial line was connected to the two Bitter coils, while for the 2-D flow accelerator wedge model tests, it is connected to the two copper electrodes.

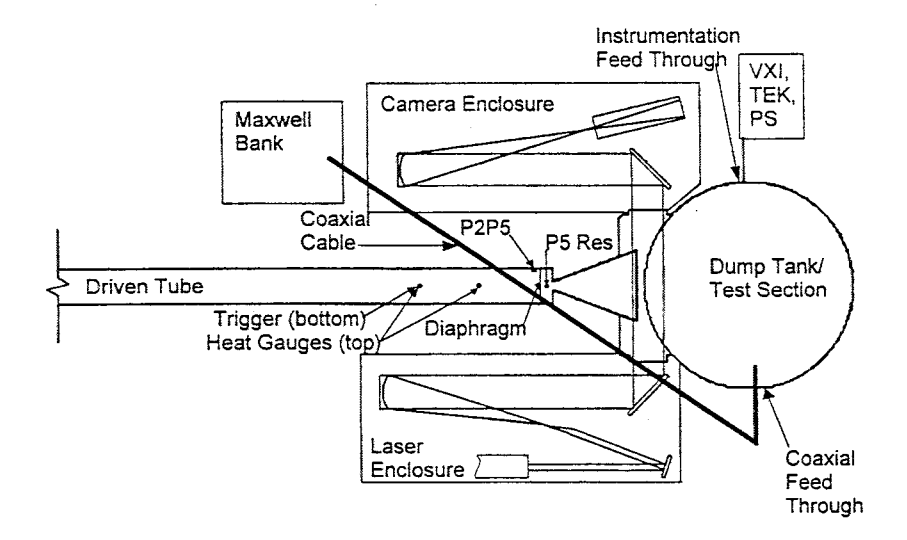


Fig. 3 Layout of the Shock Tunnel and Instrumentation

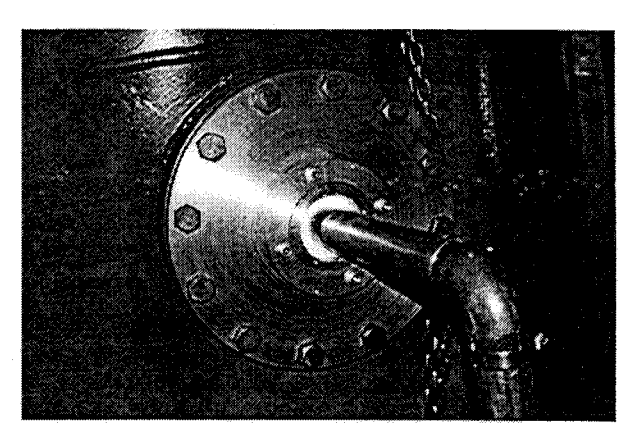


Fig. 4 Test Section Power Feed Through

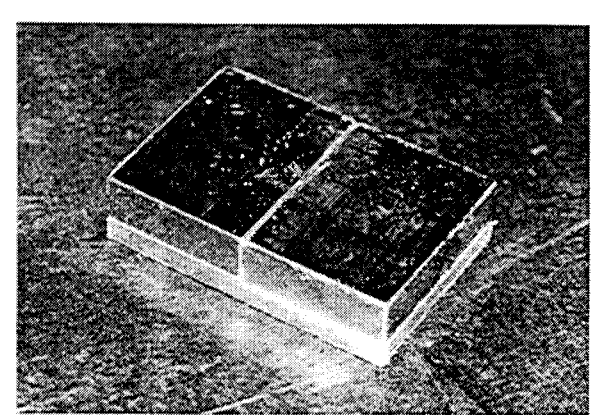


Fig. 5 Permanent Magnet Assembly

The wedge model was conceived with the idea of using the Maxwell Capacitor Bank to provide the electrode energy. It is for this reason that permanent magnets were chosen to simplify the model and free the capacitor bank. Each one of the neodymium-iron-boron magnets measures 2.0-in. X 1.5-in. X 0.5-in.; they are commercially available from Edmund Scientific. Two such magnets were glued together to create the bottom of the MHD channel, which measures 2-in. wide by 3-in. long. They were then mounted on a cold rolled steel back plate 0.25 in. thick and epoxied into a pocket machined in the wedge top surface, between the two electrodes. Figure 5 shows the two-magnet assembly prior to its installation into the wedge model.

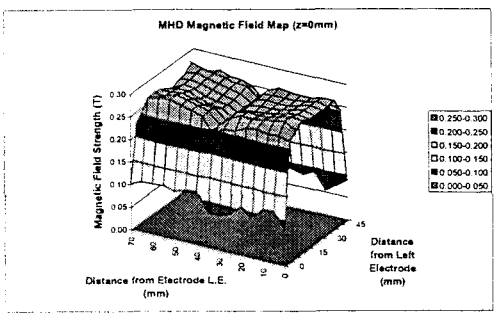


Fig. 6a Magnetic Field Strength over MHD Channel Area at z=0mm

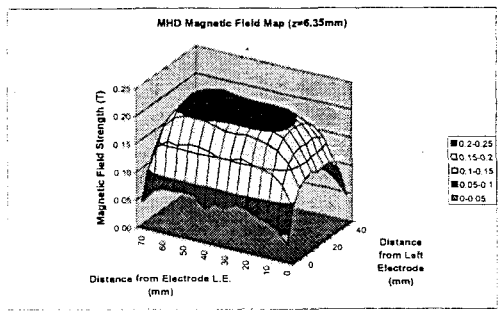


Fig. 6b Magnetic Field Strength over MHD Channel Area at z=6.35mm

A survey of the magnetic field has been completed and the field characteristics are as expected. The field is strongest at the surface and weakens with distance. At its greatest intensity near the surface of the wedge model, the magnetic field is 0.3 Tesla, and at all levels, the field strength remains roughly constant over most of the surface of the MHD channel but drops off sharply near the electrodes. Figures 6a and 6b are contours of the magnetic field strength over the MHD channel area at two heights above the wedge model surface.

Since no power is required to drive these magnets during flow deceleration and acceleration investigations, the existing capacitor bank was available to power the two solid copper electrodes. However, the discharge characteristics of the capacitor bank were determined to be too intense for the experiment at hand. Instead, a 1080 V, low current, low noise power supply was assembled using eight 540 V Eveready type 497 batteries connected to the coaxial power line. Because the 2-D model consists of a 10-in. wide wedge with a 40-degree flow deflection angle, the Mach 7.6 oblique shock wave produces a higher degree of ionization than does the oblique shock for the axisymmetric model case. In addition, because the model is symmetric with respect to the nozzle exit horizontal plane and the permanent magnet and two electrodes are installed only in the upper surface (Fig. 8), it is possible to observe both the MHD disturbed (top) and undisturbed (bottom) wedge flows in each experiment.

The Eveready battery power supply was chosen because of its high voltage ability and expected high currents during the transient. The current, however, has not been high enough in previous experiments. A lower voltage, high current battery supply has thus been envisioned with an exploding wire to start the MHD current flow. An inhouse designed and built timing circuit controls the closing and opening of the switch in Figure 7, the present power supply.

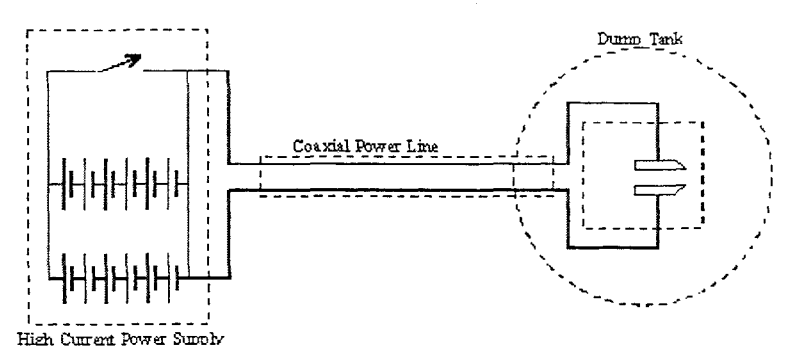


Fig. 7 Schematic of Electrode Power Supply and Delivery System

The MHD slipstream decelerator and accelerator wedge model is shown in Fig. 8. The centerline of the exit region of the MHD wedge model is instrumented with two surface pressure taps and two impact pressure probes, as diagrammed. The two impact pressure probes can be adjusted vertically to help determine the dynamic pressure distribution downstream of the MHD channel centerline. The impact pressure probes are mounted symmetrically with respect to the nozzle exit horizontal plane so that both dynamic pressures, downstream of the MHD channel (top wedge surface) and downstream of the unaffected oblique shock wave (bottom surface), can be measured simultaneously. In addition, an impact pressure rake has been recently machined to provide four pressure traces at varying heights above the wedge surface in place of either the top impact or bottom impact probe. Initial tests with this setup have provided some interesting results. impact pressure probe, located outside the model, measures the free stream pitot pressure necessary to determine the nozzle exit flow conditions. wedge material is DelrinTM, and due to its relative softness, the model was fitted with a removable DelrinTM leading edge, to allow the edge to be replaced after excessive erosion. After more than seventy runs, however, erosion of the original leading edge is still not apparent.

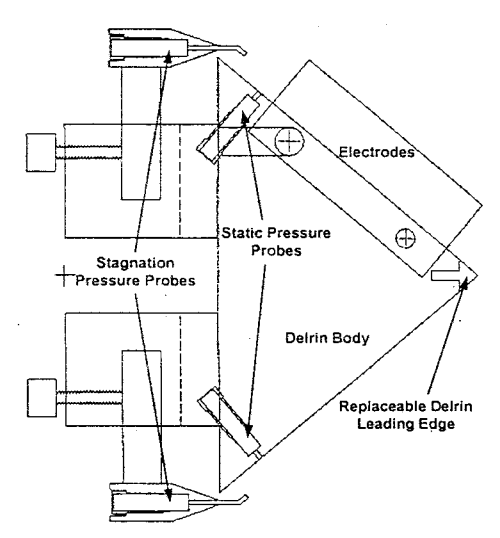


Fig. 8 MHD Slipstream Accelerator Wedge Model

As in the axisymmetric inlet model, PCB model 112A22 piezoelectric pressure transducers were used in all model probes and surface pressure taps. Because of induced noise considerations and the desire to minimize the grounding paths for the discharge, fiber optic transducers are envisioned for the project's next stage. A hollow stainless steel shaft connects the model to the test section main sting support system and carries the pressure transducer

cables to a vacuum feed-through plate. A pair of ionization gauges has also been constructed to help determine flow conductivity. The first of these is a surface mount gauge, which provides a feedback signal whenever current from an external source flows across a 1mm gap between copper conductors. The second operates on the same principle but is presently mounted off the bottom surface of the model. When exploding wire tests commence the off-surface gauge will be moved to the area behind the MHD channel.

The rectangular MHD electrodes are 0.75-in. X 3-in., 2-in. apart, and are removable to allow different electrode shapes and concepts to be tested. To minimize flow disturbances, the electrodes have sharp leading edges and the ramp surfaces face the channel's outside. Two small, 1mm diameter holes near the electrode leading edges allow the use of a copper fuse wire to start the discharge during the flow acceleration attempts. Solid threaded copper rods, under the wedge top surface, connect the electrodes to the cables that bring power from the high current power supply.

An actual photograph of the 2-D model before its installation in the Hypersonic Shock Tunnel test section is shown in Fig. 9. The single upper and lower impact pressure probes and the main pitot pressure probe are visible in this photograph.

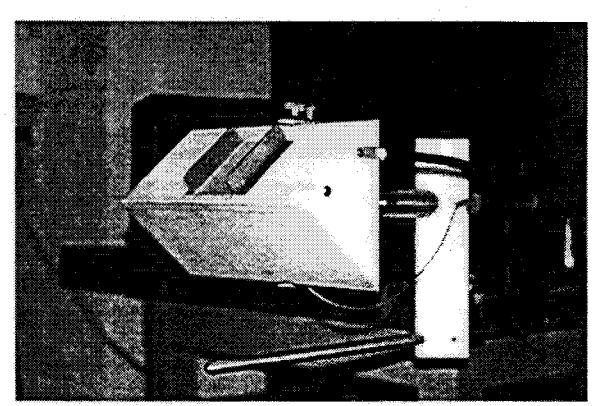


Fig. 9 2-D MHD Slipstream Accelerator Model outside the tunnel test section

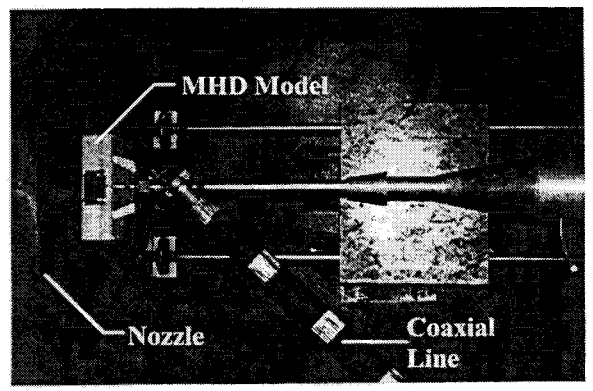


Fig. 10 2-D MHD Slipstream Accelerator Model installed in the Shock Tunnel Test Section

Figure 10 shows the model installed in the RPI facility test section. The coaxial power line that is used to deliver the high current pulse to the copper electrodes can also be seen in this figure.

AIR PLASMA CHARACTERISTICS

An iterative solver has been developed in FORTRAN by previous graduate students (Minucci, 12 1991, Messitt, 16 1999) to determine both the reservoir and freestream conditions from initial data for each run in the RPI facility. As mentioned previously, the RPI HST has been operated to produce 4100 K stagnation temperature and 780 psia stagnation pressure in the reservoir section for the present investigation. These reservoir conditions are sufficient to produce between 6 ms and 8 ms of Mach 7.6 flow in the test section. After expanding through a conical diverging nozzle, the flow static temperature and static pressure are 450 K (810 R) and 0.020 psia, respectively.

Theoretical Flow Conditions

Using NACA 1135¹⁷ (1953) and various other resources, real gas conditions in the MHD channel have been determined as accurately as possible with current real gas theories and without introducing unnecessary complexity. Boundary layers are ignored in all calculations. The conditions on the wedge and behind the oblique shock wave are:

stagnation pressure = 7.9 psia static pressure = 0.88 psia static temperature = 2992 K density = 7.369 x 10⁻³ kg/m³ Mach number = 2.3 velocity = 2082 m/s mass flow rate = 0.01580 kg/s flow power = 79.6 kW mass in channel = 0.58 mg These calculations are based on freestream conditions as follows:

stagnation pressure = 780 psia static pressure = 0.020 psia stagnation temperature = 4100 K static temperature = 450 K density = .0011 kg/m³ Mach number = 7.6

Of course, this implies that the MHD channel stagnation temperature is 4100 K.

Measured Flow Conditions

The flow conditions that have been measured differ, sometimes significantly, from theory. In most cases, the impact pressure and static pressure differ from the top to the bottom side of the wedge. In addition, the impact pressure is significantly lower than theory would have it in all cases. The experimental data suggests the following values:

channel-side stagnation pressure = 3.3 psia opposing-side stagnation pressure = 4.5 psia channel-side static pressure = 0.77 psia opposing-side static pressure = 1.2 psia

Explanations offered for the difference in pressures measured from one side to the other include a misalignment of the model and magnetic field interference with the transducers.

Gas Composition

The Chemical Equilibrium with Applications (CEA) computer code (Gordon & McBride, 18 1994) was used to determine gas composition at the conditions behind the oblique shock wave. For the given conditions, the major constituents of the hot test gas, in order of decreasing abundance, are N₂, O₂, O, NO, Ar, CO₂, CO, and other, less abundant particles, including free electrons.

Plasma Conductivity

The electrical properties of the wedge model in the flow have also been determined both experimentally and theoretically. The most important of these parameters, conductivity, has been determined entirely experimentally, because we have good reason to believe that the gas is in a state of chemical nonequilibrium, making it very difficult to calculate.

The conductivity has been determined during a series of runs with the wedge acting as a MHD generator. During these runs an external load was changed, which in turn changed the amount of current generated by the wedge. The plasma resistance changed nonlinearly with this change. When run with the highest external load, the conductivity was determined to be 5.19×10^{-5} mho/cm, while at the lowest external load, the conductivity was 3.50×10^{-3} mho/cm.

The open circuit voltage, V_0 , can be determined experimentally as the measured electromotive force that is induced with the highest external load. The experimentally determined open circuit voltage for the MHD wedge generator model in a Mach 7.6, 4100 K stagnation temperature, 780 psia stagnation pressure flow is 10.6 volts with an external load of 762.2 k Ω .

Theoretically, this open circuit voltage can be determined with the following relation (Blake, 1999):

$$V_0 = \frac{U_2 B L}{10^8}$$
 (1)

where U_2 is the plasma velocity in cm/sec, B is the magnetic field strength in gauss, and L is the electrode separation distance in cm. The theoretical value of open circuit voltage thusly determined is 32.2 volts.

Although the difference between the theoretical and experimental values of this voltage is significant, the order of magnitude is the same. The theoretical model does not account for boundary layers over either the wedge or its electrodes, electrode sheaths (Schneider²⁰, 1999), or the variation in the magnetic field strength with perpendicular distance from the surface. Considering these additional physical phenomena, all of which decrease the induced voltage, the theoretical open circuit voltage agrees fairly well with the observed open circuit voltage.

Conductivity was determined experimentally using the same method as Blake¹⁹ (1999). The plasma resistance, R_p , without any external load, can be found from the following equation:

$$V = V_0 - IR_p \tag{2}$$

where V is the measured potential between the electrodes, and the induced current, I, is found using Ohm's Law:

$$I = V/R_{ex} \tag{3}$$

where R_{ex} is the external load. The conductivity, σ , of the plasma in a channel with electrode area A and separation distance L can then be determined by

$$\sigma = \frac{L}{AR_{p}} \tag{4}$$

Using a more conservative model for theoretical open circuit voltage, the voltage drop at the electrode sheaths can be estimated. As the magnetic field drops off uniformly with distance, the average field strength at a height of 9.53mm above the surface of the wedge (approximately half the electrode height) will be used for the value of B. This value is 0.127 T. The result is a new theoretical open circuit voltage of 14.3 volts. The average extracted voltage for the three runs with highest external load was 10.6 volts.

Equation 5 is a form of eq. 2, modified to include the contribution of the electrode sheaths.

$$V = V_0 - V_e \tag{5}$$

Where V is the average measured voltage given above, V_0 is the theoretical open circuit voltage, and V_e is the combined voltage drop at the electrode sheaths. Using this method, the voltage drop at the electrode sheaths is determined to be approximately 3.7 volts.

ADDITIONAL GENERATOR RESULTS

Most of the generator results for the primary stage of the investigation were presented by Minucci²¹ et al. (2000). To help verify the results and check the model setup after reinstallation, however, some additional conditions were run in the generator mode. These conditions were chosen to help better define the regions between the generator behavioral regimes. Figures 11a through 11d are the updated generator performance plots and make obvious these different regimes.

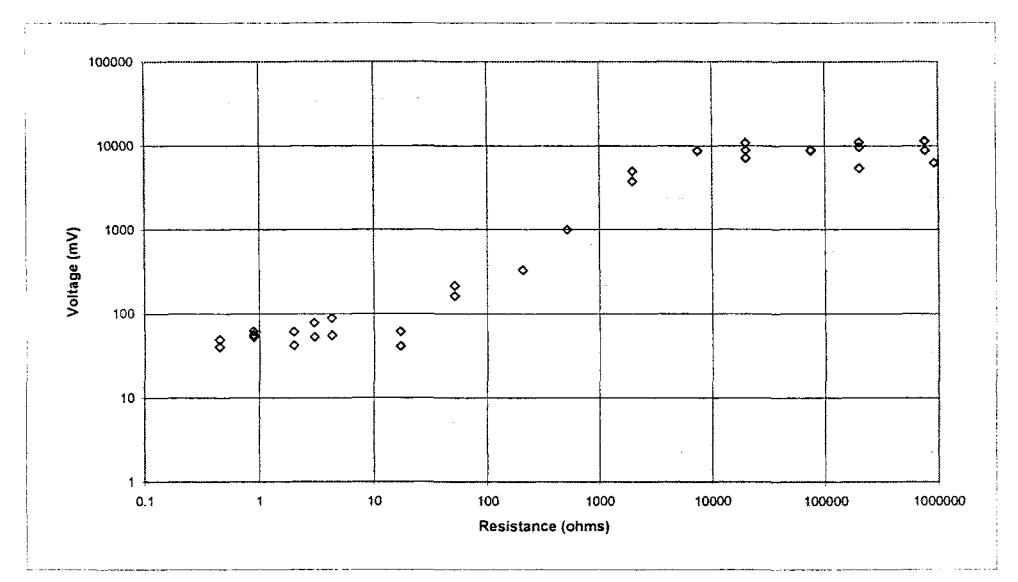


Fig. 11a Potential Across Electrodes as a Function of External Resistance

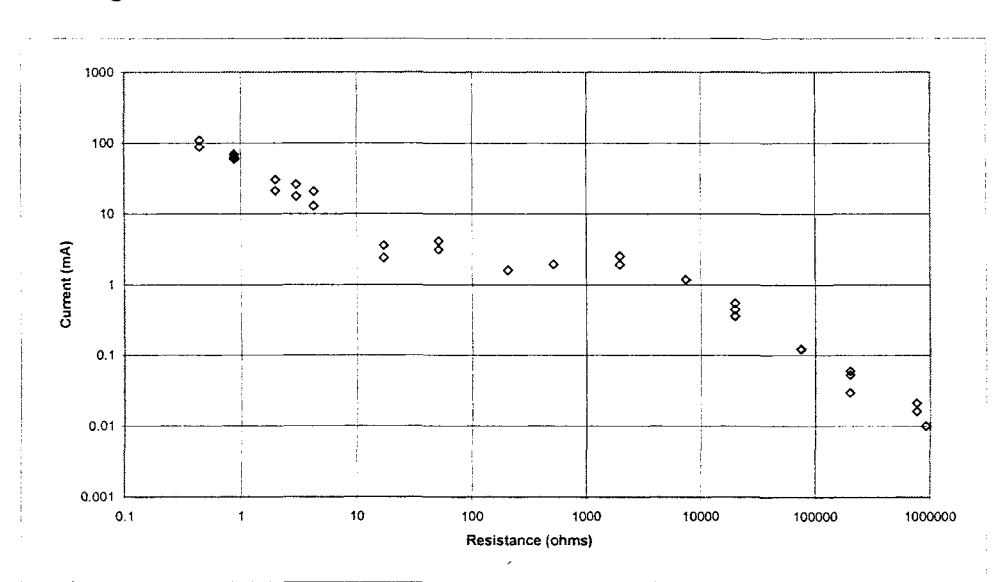


Fig. 11b Electric Current Output as a Function of External Resistance

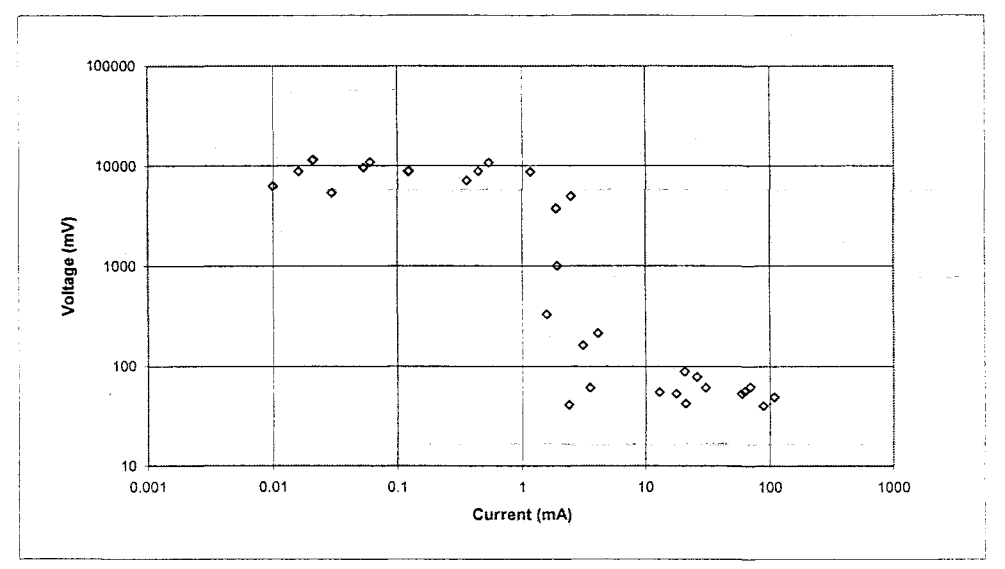


Fig. 11c Potential across Electrodes as a Function of Electric Current Output

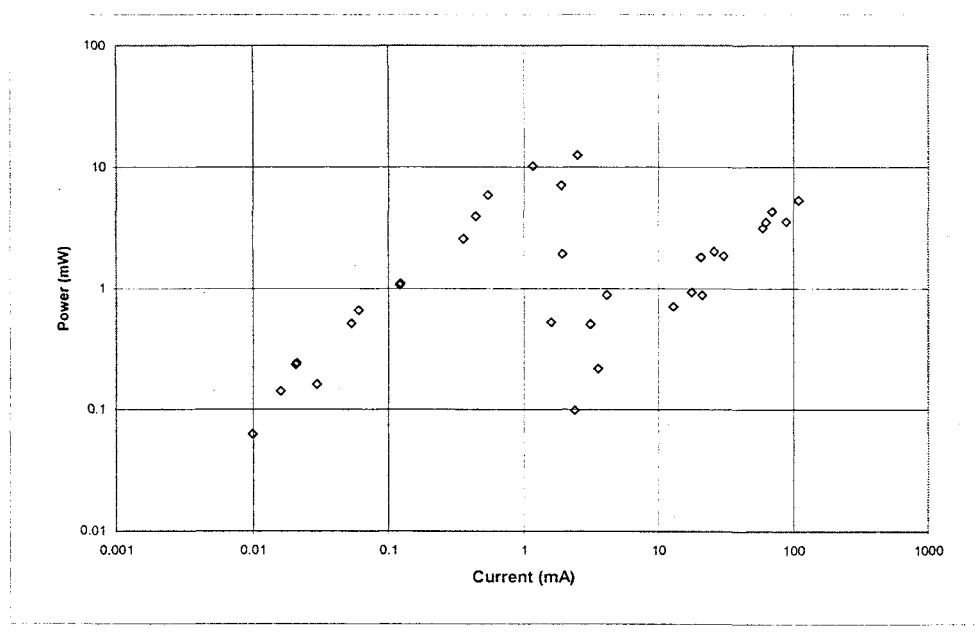


Fig. 11d Power Output as a Function of Electric Current Output

The six additional conditions tested all seem to fit in well with the past data, thereby greatly increasing confidence in the accuracy of the data.

The greatest power extracted from the generator at any time was 12.5 mW. Given a flow power of 79.6 kW, this implies an extraction efficiency of 1.6×10^{-5} %. This low extraction efficiency can again be attributed to low conductivity and high impedance at the electrode sheaths.

EXPLODING WIRE CONCEPT

At 3000 K static temperature the equilibrium conductivity of air is negligible. The experimentally

determined conductivity is nonzero primarily due to nitrogen species frozen in their reservoir state. Many methods, therefore, have been envisioned to artificially increase the flow conductivity. These methods include seeding, exploding trigger wires, high voltage discharges, and laser- or microwave-induced breakdown. For the next phase of the MHD wedge accelerator investigation, exploding trigger wires are to be used to drastically increase conductivity and to create a "T-layer" or "paddle," as described by Myrabo et al. (1995), to essentially push the air through the MHD channel.

Although the MHD accelerator design calls for a laser- or microwave-induced line breakdown, the trigger wire is a good simulator of this event. The

trigger wire concept has a number of distinct advantages over the others mentioned. It is simple and lends itself well to the current model design. The power supply and timing circuit are also easily implemented with the Hypersonic Shock Tunnel's current setup. Finally, the conductivity is expected to increase drastically as vaporized metal particles are entrained by the flow. Figure 12 is a schematic representation of what the exploding wire is expected to look like in a static environment.

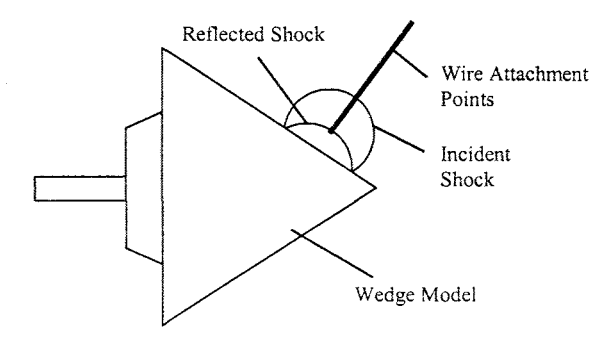


Fig. 12 Schematic of Exploding Wire Concept

When considering such an experiment, however, one has to take into account the many influences presented. Once a high current discharge has been established through the use of a trigger wire, an acceleration of the air due to the MHD effect is sure to ensue. How does one distinguish the pressure increase due to the MHD acceleration from that due to the added mass and possible shock wave contributions of the wire itself? Somehow a baseline must be established.

A second wedge model is currently being machined at RPI; it is identical to the first in every way except that the magnet has been omitted. By establishing a discharge across the electrodes of this second, magnetless model in the flow, therefore, we can establish a baseline impact pressure measurement for the experiments. Further results obtained with the magnet-equipped model can then be compared to the baseline results.

While proper wire size and composition is being decided upon, some initial estimates of mass can be made. An expectedly 5.4 cm long, one-half milligram wire may add significantly to the calculated mass flow rate of 15.8 g/s. Copper wire could prove an interesting choice, as the excited vaporized copper atoms may interact with the copper vapor laser beam in some uncertain way. It could either absorb energy, leaving a dark spot on the schlieren photos, or possibly serve as a short, one-pass amplifier to overexpose portions of the photos. It is for these reasons that copper may also not be the best choice for wire material

FUTURE WORK

Calculations show that at 100% efficiency, an applied power of 30.2 kW should create a 1 psia impact pressure increase in the MHD channel flow. The current in this case should be as high as possible, somewhere on the order of 400 amps assuming, again, 100% efficiency. Of course, we cannot expect anywhere near 100% efficiency, but this gives us some estimate of our power requirements.

Five, 1000 amp lead-acid batteries will provide 63 kW at anywhere from 1 kA to 5000 kA. With this sort of power supply, the new "T-layer" approach, and the possibility of a redesigned model, we expect to see useful MHD accelerator results.

SUMMARY AND CONCLUSIONS

- All experiments to date with the MHD generator have been performed with ambient levels of conductivity over an 80-degree included angle wedge model.
- Experiments characterizing the physics of this MHD slipstream generator without augmenting air plasma conductivity have been completed.
- The extraction efficiency of this device is not beneficial to propulsion applications, but the device has proven a useful diagnostic tool for flow conductivity.
- An extremely useful tool for studying fast transient events has been developed: schlieren movies at 10-30 kHz can be created with a drum camera, 30 kHz Cu-vapor laser, and controllers.
- Fiber optic transducers will likely be required to obtain data of satisfactory quality with negligible noise.
- A high current, low voltage, stable DC source is being assembled of lead-acid batteries.
- The next stage in experimentation is the testing of MHD slipstream accelerators that employ pulsed "T-layers."
- The T-layer approach maximizes the percentage of input energy used to accelerate the flow by minimizing the energy used to simply enhance flow conductivity.
- This concept has been traditionally proposed for laser and microwave Lightcraft.

ACKNOWLEDGEMENTS

This report is being prepared under Grant No. NAG8-1290 from NASA Marshall Space Flight Center. The donation of the Maxwell capacitor bank

and the accompanying control cabinet by the US Army Picatiny Arsenal is gratefully acknowledged. Also, the second author would like to acknowledge the support for his Post-doctoral Program at the Rensselaer Polytechnic Institute from the Brazilian Air Force. Finally, the authors would like to acknowledge the important contributions to this project from K. Shanahan, R. Nolan, A. Zielinski, J.M. Kerl, A.D. Panetta, D.G. Messitt, and C. Vannier.

REFERENCES

- Rosa, R.J., "Magnetohydrodynamic Generators and Nuclear Propulsion," ARS Journal, August, 1962, pp.1221-1230.
- Nagamatsu, H.T., and Sheer, R.E.Jr., "Magnetohydrodynamics Results for Highly Dissociated and Ionized Air Plasma," *The Physics of Fluids*, Vol. 9, September 1961, pp.1073-1084.
- 3. Nagamatsu, H.T., Sheer, R.E. Jr., and Weil, J.A., "Non-Linear Electrical Conductivity of Plasma for Magnetohydrodynamic Power Generation," ARS Paper 2632-62, November 1962.
- 4. Way, S., DeCorso, S.M., Hundstud, R.L., Kenney, G.A., Stewart, W., and Young, W.E., "Experiments with MHD Power Generation," Trans. Am. Soc. Mech. Eng., J. Eng. Power 83, Series A. October 1961, pp.394-408.
- 5. Steg, L. and Sutton, G.W., "The Prospects of MHD Power Generation," *Astronautics 5*, August 1960, pp.22-25.
- Ericson, W.B., Maciulaitis, A., Spagnolo, F.A., Loefler, A.L. Jr., Scheuing, R.A., and Hopkins, H.B. Jr., "An Investigation of MHD Flight Control," Grumman Aircraft Engineering Corp., National Electronics Conference, Dayton, Ohio, May, 14-16, 1962.
- 7. Covault, G. "'Global Presence' Objective Drives Hypersonic Research," *Aviation Week & Space Technology*, April 5, 1999, pp. 54-58.
- 8. Gurijanov, E.P., Harsha, P.T. "AJAX: New Directions in Hypersonic Technology," AIAA Paper 96-4609, 1996.

- Myrabo, L.N., Mead, D.R., Raizer, Y.P., Surzhikov, and Rosa, R.J., "Hypersonic MHD Propulsion System Integration for a Manned Laser-Boosted Transatmospheric Aerospacecraft," AIAA Paper, June 1995.
- Kerl, J.M., Myrabo, L.N., Nagamatsu, H.T., Minucci, M.A.S., and Meloney, E.D., "MHD Slipstream Accelerator Investigation in the RPI Hypersonic Shock Tunnel,"
 AIAA Paper 99-2842, July 1999.
- 11. Kerl, J.M., Myrabo, L.N., Nagamatsu, H.T., Minucci, M.A.S., and Meloney, E.D., "MHD Slipstream Accelerator Investigation in the RPI Hypersonic Shock Tunnel," Rensselaer Polytechnic Report for NASA Marshall Space Flight Center, Grant No. NAG8-1290, July 15, 1999.
- 12. Minucci, M.A.S., "An Experimental Investigation of a 2-D Scramjet Inlet at Flow Mach Numbers of 8 to 25 and Stagnation Temperatures of 800 to 4.100 K, "Ph. D. Thesis Dissertation, Department of Mechanical Engineering, Aeronautical Engineering & Mechanics, Rensselaer Polytechnic Institute, Troy, New York, USA. May 1991.
- 13. Minucci, M.A.S., Nagamatsu, H.T., "Hypersonic Shock-Tunnel Testing at an Equilibrium Interface Condition of 4100 K," *Journal of Thermophysics and Heat Transfer*, Vol. 7, No. 2, 1994, pp. 251-260.
- 14. Nascimento, M.A.C., "Gaseous Piston Effect in Shock Tube/Tunnel When Operating in the Equilibrium Interface Condition," Ph.D. Thesis Dissertation, Instituto Tecnologico de Aeronautica – ITA, Sao Jose dos campos, Sao Paulo, Brazil, October 1998.
- 15. Nascimento, M.A.C., Minucci, M.A.S., Ramos, A.G., and Nagamatsu, H.T., "Numerical and Experimental Studies on the Hypersonic Gaseous Piston Shock Tunnel," *Proceedings of the 21st International Symposium on Shock Waves*, September 1997.
- 16. Messitt, D.G., "Computational and Experimental Investigation of 2-D Scramjet Inlets and Hypersonic Flow over a Sharp Flat Plate," Ph. D. Thesis Dissertation, Department of Mechanical Engineering, Aeronautical Engineering & Mechanics, Rensselaer

- Polytechnic Institute, Troy, New York. May 1999.
- 17. Ames Research Staff, "Equations, Tables, and Charts for Compressible Flow," NACA Report 1135, 1953.
- 18. Gordon, S. and McBride, B., "Computer Program for Calculation of Complex Chemical Equilibrium Compositions and Applications," NASA RP-1311, 1994.
- Blake, S., "Magnetohydrodynamic Results for Highly Dissociated and Ionized Air Plasma for Mach 30 and 11,600 K," M.S. Thesis Dissertation, Rensselaer Polytechnic Institute, August 1999.
- Schneider, M.N., Macheret, S.O., and Miles, R.B., "Electrode Sheaths and Boundary Layers in Hypersonic MHD Channels," AIAA Paper 99-3532, July, 1999.
- 21. Minucci, M.A.S., Meloney, E.D., Nagamatsu, H.T., Myrabo, L.N., and Bracken, R.M., "Experimental Investigation of a 2-D MHD Slipstream Generator and Accelerator with $M_{\infty} = 7.6$ and $T_0 = 4100$ K," AIAA Paper 00-0446, January 2000.